

Neutron-Star Radius from a Population of Binary Neutron Star Mergers

Sukanta Bose,^{1,2,*} Kabir Chakravarti,¹ Luciano Rezzolla,^{3,4} B. S. Sathyaprakash,^{5,6,7} and Kentaro Takami^{8,3}

¹*Inter-University Centre for Astronomy and Astrophysics, Post Bag 4, Ganeshkhind, Pune 411 007, India*

²*Department of Physics & Astronomy, Washington State University, 1245 Webster, Pullman, Washington 99164-2814, USA*

³*Institut für Theoretische Physik, Max-von-Laue-Straße 1, 60438 Frankfurt, Germany*

⁴*Frankfurt Institute for Advanced Studies, Ruth-Moufang-Straße 1, 60438 Frankfurt, Germany*

⁵*Institute for Gravitation and Cosmos, Physics Department, Pennsylvania State University, University Park, Pennsylvania 16802, USA*

⁶*Department of Astronomy & Astrophysics, Pennsylvania State University, University Park, Pennsylvania 16802, USA*

⁷*School of Physics and Astronomy, Cardiff University, 5, The Parade, Cardiff CF24 3AA, United Kingdom*

⁸*Kobe City College of Technology, 651-2194 Kobe, Japan*



(Received 29 May 2017; revised manuscript received 4 October 2017; published 16 January 2018)

We show how gravitational-wave observations with advanced detectors of tens to several tens of neutron-star binaries can measure the neutron-star radius with an accuracy of several to a few percent, for mass and spatial distributions that are realistic, and with none of the sources located within 100 Mpc. We achieve such an accuracy by combining measurements of the total mass from the inspiral phase with those of the compactness from the postmerger oscillation frequencies. For estimating the measurement errors of these frequencies, we utilize analytical fits to postmerger numerical relativity waveforms in the time domain, obtained here for the first time, for four nuclear-physics equations of state and a couple of values for the mass. We further exploit quasiuniversal relations to derive errors in compactness from those frequencies. Measuring the average radius to well within 10% is possible for a sample of 100 binaries distributed uniformly in volume between 100 and 300 Mpc, so long as the equation of state is not too soft or the binaries are not too heavy. We also give error estimates for the Einstein Telescope.

DOI: 10.1103/PhysRevLett.120.031102

Introduction.—The direct observation of gravitational waves (GWs) by LIGO [1] has increased the expectation that advanced GW detectors will also detect other types of binaries, including binary neutron stars (BNSs). Imprinted in the GWs emitted by BNSs is the signature of the equation of state (EOS) of nuclear matter. This signature manifests itself during the inspiral phase, when the two stars are tidally deformed [2], and in the postmerger, when an unstable hypermassive neutron star (HMNS) can form, emitting GWs at characteristic frequencies [3–5]. In both cases, however, these imprints will be extremely small, and the accuracy of measurement of EOS parameter(s) will be poor, even in detectors like Advanced LIGO (aLIGO) [6] and Advanced Virgo (AdV) [7], unless the binary happens to be nearby.

One way to address this problem is to combine the information in multiple observations [8] with the expectation that the EOS parameter errors will reduce as the number of observations increases. For instance, the error in the tidal deformability parameter can go down as fast as the inverse square root of the number of BNS detections [9,10]. However, several tens of observations are needed to reduce the errors to a level where only extreme EOSs can be distinguished. An alternative method is to measure the characteristic frequencies of the merger and postmerger signals [4,11–14]; e.g., the frequency at the amplitude’s maximum, f_{\max} , correlates closely with the tidal deformability of the

two stars [13,15,16], and the spectrum of the postmerger GW signal exhibits at least three strong peaks of increasing frequency, dubbed f_1 , f_2 , and f_3 [12,13].

In this Letter, we explore how well the radius of a neutron star can be measured by utilizing both the inspiral and postmerger phases of the signal from multiple observations. For this purpose, we utilize numerical relativity (NR) simulations to devise an analytical model of the postmerger waveforms of four reference nuclear-physics EOSs (ALF2, SLy, H4, and GNH3; see Ref. [13] for details) in terms of a linear superposition of damped signals with characteristic frequencies f_1 and f_2 . The model allows us to estimate errors $\Delta f_{1,2}$, which are very large for individual observations in aLIGO or AdV, as the signal-to-noise ratio (SNR) of postmerger oscillations is $\lesssim 1$ for a source at ~ 200 Mpc. However, the joint error, e.g., in f_2 , for a population of ≈ 100 BNSs, uniformly distributed in the comoving volume between 100 Mpc and 300 Mpc, and observed in the aLIGO-AdV three-detector network, is a few to several percent, depending on the EOS. In essence, for a given binary with average mass \bar{M} and average radius at infinite separation \bar{R} , the quasiuniversal relations between the characteristic frequencies f_1 and f_2 and compactness $C := \bar{M}/\bar{R}$ [13,17] can be used to deduce the error in C from the errors in those frequencies, for various masses and mass ratios. (While our analysis utilizes these relations, it is not

affected by how strictly universal they are.) Such measurement of \mathcal{C} can be combined with that of the total mass from the inspiral to estimate the average radius for a BNS population. We show that for these ≈ 100 BNS observations, the error in radius is 2%–5% for stiff EOSs and 7%–12% for soft EOSs. Our conclusion is that advanced detectors can help discriminate between stiff and soft EOSs. However, distinguishing between two stiff EOSs will be harder, with additional difficulties for very soft EOSs, whose postmerger signals are considerably weaker.

With important differences, our conclusions broadly agree with those presented recently by other groups. Agathos *et al.* [10] estimated the evolution of the medians and 95% confidence intervals in the measurement of the leading-order term c_0 in the expansion of the tidal deformability at the reference mass of $1.35 M_\odot$, for some reference EOSs in simulated aLIGO data [10] and a Gaussian mass distribution. They found that inspiral signals from ≈ 100 or more BNSs are required for determining c_0 to 10% accuracy. Our analysis is different, in that instead of constructing Bayesian posteriors of c_0 from the inspiral waveform, we use Monte Carlo simulations to estimate the radius, but require a similar number of sources for discriminating similar pairs of EOSs.

Clark *et al.* [18] have instead used principal-component analysis to infer the postmerger waveform in various planned or proposed detectors and deduced that in aLIGO the radius of a BNS at a distance of 30 Mpc and with component masses of $1.35 M_\odot$ each can be estimated to within 430 m, which is a 3%–4% error. This result appears to agree with our strong-signal case discussed below up to a factor of 2. However, their estimates of the postmerger amplitudes are likely affected by the use of more dissipative numerical methods than those employed here and by an approximate treatment of general relativity. We also account for the deterioration in the measurement arising from covariances of BNS masses and the postmerger frequencies values, on the one hand, and the improvement in estimation accuracy that can be had from knowledge of the total mass from the inspiral phase, on the other hand.

The rate of BNS mergers remains rather uncertain, with estimates ranging from 20 in five years [19–21] to 50–100 in two to three years [8,22] in aLIGO-AdV, none of which is currently ruled out [23]. This is why we present here radius error estimates for 20, 50, and 100 detections.

Postmerger waveforms.—NR simulations have shown that the most likely product of a BNS merger is a metastable HMNS that exists for several tens of milliseconds before collapsing to a black hole [5]. The GWs emitted from such an oscillating, bar-shaped object show a strong correlation with the stiffness of the nuclear material, and hence with the EOS [5]. In addition to its dependence on the total mass, mass ratio, and EOS, the postmerger GW signal has robust spectral features with prominent peaks at increasing frequencies f_1 , f_2 , f_3 . These peaks are reminiscent of spectral lines in atomic transitions [24], so that imprinted in the spectrum of the postmerger signal is the state of dense, nuclear matter.

It is generally accepted that the most prominent peak, f_2 (see Fig. 1), reflects the spin frequency of the $m = 2$ -deformed HMNS, while the origin of the broader f_1 peak is still under debate. The fact that the f_1 peak is short lived, disappearing after a few milliseconds, and is accompanied by a symmetric peak at even larger frequencies $f_3 \sim 2f_2 - f_1$, supports the interpretation that it is a transient signal produced right after the merger by the damped collisions of the two stellar cores (see Refs. [13,17] for a toy model).

Accurate modeling of waveforms from BNSs requires computationally formidable NR calculations. Since we are interested in constraining EOS parameters with extensive Monte Carlo simulations of signals from ≈ 100 binaries with various EOSs, independent noise realizations, and average measurements over hundreds of BNS population realizations, it is clear that the accuracy and costs of the NR calculations need to be traded with a less accurate but computationally efficient description of the waveforms. Hence, we have derived a phenomenological model for the postmerger waveform using analytical fits in the time domain to a catalogue of NR waveforms [13,17] that can be expressed as a superposition of damped sinusoids with a time-evolving instantaneous frequency [18,25]: $h_+(t) = \alpha \exp(-t/\tau_1) [\sin(2\pi f_1 t) + \sin(2\pi(f_1 - f_{1e})t) + \sin(2\pi(f_1 + f_{1e})t)] + \exp(-t/\tau_2) \sin(2\pi f_2 t + 2\pi\gamma_2 t^2 + 2\pi\xi_2 t^3 + \pi\beta_2)$. Here, $t = 0$ refers to the merger time, $f_{1e} = 50$ Hz, and the ansatz reproduces all of the postmerger “+” polarization signals, up to an overall amplitude; this is to be contrasted with the ansatz considered in Ref. [25], which models the waveforms only after the amplitudes have decayed to half of the initial values. (Better matches can be obtained by including more terms and parameters in the ansatz; however, the main effect of a less than perfect match is a lower SNR; see also Ref. [26] for an alternative ansatz.) The above fit agrees very well not only with the signal spectra near f_1 and f_2 , but also with the signal phase in the time domain, giving matches of $\sim 80\%$ – 94% . Therefore, when combined with a semianalytical model of the inspiral waveform, e.g., via a post-Newtonian expansion with tidal corrections, the fitting ansatz gives a complete analytic description of the signal from merging BNSs. The above fit, parametrized by eight parameters (see Table I in the Supplemental Material [27]), produces an accurate representation of the waveform phase and a reasonably good description of its amplitude. The top panels in Fig. 1 show NR amplitudes $h_+(t)$ and the analytical fits for four different EOSs and for sources at 50 Mpc. The bottom panels show the corresponding spectral amplitudes, $2\sqrt{f}|\tilde{h}(f)|$, and the sensitivity curves of aLIGO and the Einstein Telescope [28]. Here $\tilde{h}(f)$ is the Fourier transform of $h_+(t)$.

Two remarks are in order: First, the four EOSs chosen provide a good coverage of the plausible range in stiffness of nuclear matter but do not represent very soft EOSs, such as APR4 [29]. The corresponding postmerger signal is much more complex [13,17], with beats between different frequencies not reproduced with our simple fitting ansatz.

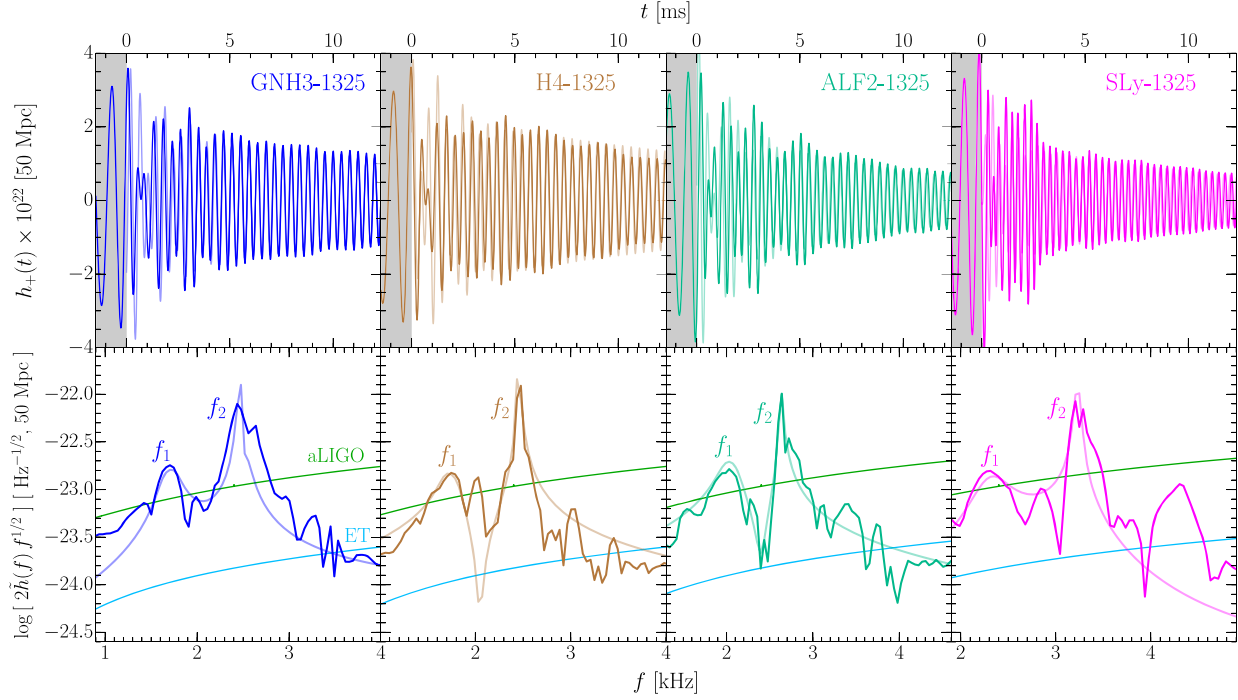


FIG. 1. *Top panels:* Postmerger strain from NR waveforms for four EOSs and a representative mass of $\bar{M} = 1.325 M_{\odot}$; our analytical ansatz is shown as a transparent line of the same color. Only the initial 12 ms of the complete 25 ms waveforms are reported to aid the comparison. *Bottom panels:* Corresponding spectral amplitudes shown with the same color convention, superposed on the strain sensitivity curves of aLIGO and the Einstein Telescope (ET) [28]. Similarly good matches are produced also for $\bar{M} = 1.250 M_{\odot}$ (cf. Table I and Fig. 3 in the Supplemental Material [27]).

Second, our fits best represent equal-mass systems, and although the masses in observed binaries do not differ significantly, it is unlikely that LIGO sources have mass ratio $q = 1$. Nevertheless, the quasiuniversal relations used here continue to be valid also for systems with mass ratio $q \gtrsim 0.8$ [13,17].

Our analytic waveforms also facilitate the interpretation of the Monte Carlo results described below in terms of the Fisher information matrix parameter estimates, which broadly agree with the former (see Table I in the Supplemental Material [27]), except for the soft EOSs. (The Monte Carlo studies are significant, since Fisher estimates, on their own, cannot be trusted when the SNR is not very high.) For a source even at 50 Mpc, the postmerger signal alone will be difficult to *detect* in an aLIGO-like detector. As an example, the postmerger waveform of the H4 binary with average mass $1.325 M_{\odot}$ (H4-1325) has $|2\tilde{h}(f)f^{1/2}| \approx 10^{-22}/\sqrt{\text{Hz}}$ at $f = f_2 \approx 2470$ Hz, with the frequency bin-width being $\delta f \sim 100$ Hz. The aLIGO noise amplitude at this frequency is $S_h(f_2) \approx 1.26 \times 10^{-46} \text{ Hz}^{-1}$, thus yielding an $\text{SNR} \approx |2\tilde{h}(f)f^{1/2}|[\delta f/(fS_h(f))]^{1/2} \approx 1.8$.

A small postmerger SNR, however, does not necessarily imply that the observations contain no information. Rather, small-SNR postmergers can provide constraints if combined constructively over a population of such signals. As an example, a Fisher-matrix analysis gives the $1 - \sigma$ error in measuring f_1 and f_2 for a population of 100 H4-1325 BNSs at 100 Mpc with optimal sky position and orientation to be

$\Delta f_1/f_1 \approx 10\%$ and $\Delta f_2/f_2 \approx 1\%$, respectively, or $\Delta f_1 \approx 177$ Hz and $\Delta f_2 \approx 27$ Hz in a single aLIGO detector (see Table I in the Supplemental Material [27]). Exploiting the quasiuniversal relations between f_1, f_2 , and the compactness (see the left two panels in Fig. 2 in the Supplemental Material [27]), we can infer the error in \mathcal{C} through error propagation. For the aforementioned 100 BNS observations, we deduce from the error in f_2 (which is much better measured than f_1) that the fractional error in the measurement of the compactness is as small as $\approx 1.0\%$. Similar results are obtained for the other EOSs and masses, and are listed in Table I in the Supplemental Material [27]. These make the case, e.g., for a thorough Monte Carlo investigation.

Radius measurement from a single BNS.—For the H4-1325 BNS at 30 Mpc, optimally oriented and located in the sky, the complete inspiral-merger-postmerger $\text{SNR} \approx 211$, even though the postmerger $\text{SNR} \approx 6.4$, in the aLIGO-AdV network. (Averaging over sky locations and orientations will reduce these SNRs by a factor of 2.26 [8,30].) At such a distance, the error in average binary mass is much smaller, at 0.08%, and $\Delta\mathcal{C}/\mathcal{C} \approx 0.9\%$. In this strong-signal case, the radius error reduces to 0.9%, or 125 m. In a single aLIGO detector, the error will rise to ≈ 215 m. This is roughly 2 times more accurate than the value given in Ref. [18], the primary reason being that their waveforms are more rapidly damped than ours, as noted above. Furthermore, while our errors are estimated for the average radius of the parent BNS, the error in Ref. [18] is estimated for the radius of a

cold nonrotating neutron star of mass $1.6 M_{\odot}$ ($R_{1.6}$) and for a single value of the average mass ($\bar{M} = 1.350 M_{\odot}$); we find this approach not applicable to our data or that of other groups (see Fig. 5 in the Supplemental Material [27]).

Radius measurement from a BNS population.—At such small SNRs, it is not possible to measure $f_{1,2}$ accurately. However, for a population of $N > 1$ BNSs it is possible to align and stack the f_2 peaks, so that for a large enough N , and uncorrelated noise across those N observations, the stacked amplitude spectra can have enough SNR to allow for an accurate measurement of f_2 . A realistic population will have a variety of mass pairs, but since the total mass of a BNS system correlates well with f_2 [17,31], one can use a measurement of $M_{\text{tot}} = 2\bar{M}$ from the inspiral waveform to deduce it. To test this idea, we performed a Monte Carlo simulation (see Supplemental Material [27]) comprising multiple time series, each with a simulated postmerger signal from this BNS population added to Gaussian noise with aLIGO zero-detuned high-power (ZDHP) noise power spectral density (PSD) [32] for all three detectors. Similar to Ref. [18], we rescaled the multiple signal spectra to align the f_2 values deduced from the (generally erroneous) total mass estimate for each signal to stack all at a chosen common frequency, f_2^c . Standard spectral frequency estimation yielded the value of f_2^c and its statistical spread for that population. We next used the quasiuniversal relation between f_2 and compactness, and error propagation, to deduce the error in the neutron-star radius of that population for any given EOS.

Since the mass distribution of extragalactic BNSs is not known, we study two different populations. In the first case, we took the masses to be uniformly distributed in a range listed below. In the second case, we built a large set of normally distributed masses centered at $1.35 M_{\odot}$, with standard deviation $0.05 M_{\odot}$, to mimic the masses in galactic BNSs [10]. We then drew our sample of $2N$ masses from this distribution by restricting them to lie within a given range.

For all EOSs and the two mass distributions (Gaussian and uniform), the radius errors found from Monte Carlo studies are similar to those obtained from Fisher studies, provided one limits the masses to the range $[1.2, 1.38]M_{\odot}$ (see Fig. 2). As an example, observations of 100 BNSs in aLIGO with Gaussian mass distribution will measure the radius with a 5% accuracy for ALF2 (at 90% confidence). The same set observed by the Einstein Telescope (ET) [28] will measure it with an accuracy of 0.7%; for other EOSs, the error in ET is a factor of ≈ 7 smaller than the corresponding aLIGO values shown in Fig. 2.

A notable departure from the Fisher estimates in Fig. 2 is the error for the Gaussian mass distribution with the SLy EOS. The reason for the agreement with the Fisher-matrix estimates elsewhere is that the average value of f_2 is not very high. However, for the Gaussian mass distribution for SLy, the average f_2 is the highest, so that for the same percentage error in f_2 , the error Δf_2 is largest for SLy. This implies that the stacking of signals works less perfectly and

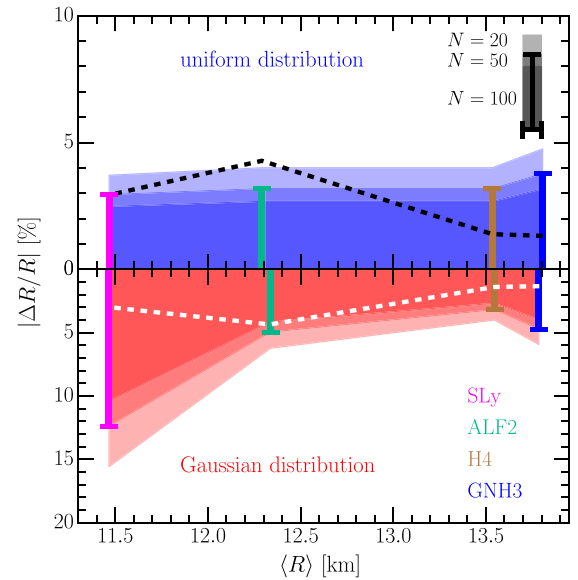


FIG. 2. Estimated relative error in the radius measured, at 90% confidence level, versus the average population radius for different EOSs and $N = 20, 50, 100$ (different shadings) BNSs distributed uniformly in a comoving volume between 100 and 300 Mpc. The two panels refer to binaries whose distribution in mass in the range $[1.2, 1.38]M_{\odot}$ is either uniform (top) or Gaussian (bottom). Shown with dashed lines are the errors from the Fisher-matrix analysis for $N = 50$.

the summed signal at the fiducial frequency grows more slowly with the number of observations than what is realized in the Fisher method. To confirm this behavior, we performed two Monte Carlo simulations with 100 BNSs each, one with all neutron-star masses $= 1.25 M_{\odot}$ and another with all of them $= 1.325 M_{\odot}$. For the SLy EOS, the radius error is $\approx 2.7\%$ for the first (low-mass) case, but rises to $\approx 10\%$ for the second case, at 90% confidence.

From Fig. 2, it is clear that as the EOS gets softer, the Fisher-matrix errors will be less credible. If the EOS turns out to be soft, then measuring the radius to an accuracy of 10% will be challenging with aLIGO-like detectors.

Conclusions.—We have presented a new method to infer the average radius of a population of neutron stars in BNSs that employs both the inspiral-merger and the postmerger phases. The postmerger allows for the measurement of the compactness, which complements the measurement of the component masses from the inspiral to determine the radius. Our modeling of the postmerger can help produce complete inspiral, merger and postmerger time-domain waveforms.

It may be argued that our results are somewhat limited for a couple of reasons. First, our phenomenological fits and the estimates of the errors $\Delta f_{1,2}$ are given for binaries with mass ratio $q \approx 1$. However, we have found that similar fits can be obtained for unequal mass ratios studied in Ref. [17], and that $\Delta f_{1,2}$ are very similar in such cases for signals with the same SNRs. This observation is consistent with those made in Ref. [18]. If nature relents to provide us with an especially strong signal, such that the network SNR of the postmerger

signal is ≈ 6.4 , which can happen if the source is of optimal orientation and sky position and located at a distance of 30 Mpc, then our method can be used to deduce the radius to about 1.6%, at 90% confidence level. Second, as the number of observed binaries increases and the fractional errors of the EOS properties decrease, the systematic uncertainties, mostly related to the accuracy of NR calculations, will dominate. The average numerical error from the simulations is ~ 0.1 kHz, while the average uncertainty for the identification of peak frequencies is ~ 0.2 kHz [13,24]. Third, we ignored the effect of spins, which can increase the total-mass error [33], and therefore the effectiveness of the stacking method. They can also change f_2 by 0.2–0.3 kHz in the most extreme cases [34,35]. While this is comparable to the NR uncertainty, it is important that spin effects be properly incorporated in future simulations. (For more details on the quasiuniversal relations and parameter-estimation methods employed in this work, see the Supplemental Material [27], which includes Refs. [36–39].) Finally, since both the imprint of EOS and the signals themselves may be weak, it will be important to utilize as much of the signal as is meaningful for measuring the EOS parameters. This can be especially helpful owing to the possibility that these parameters may have nontrivial covariances with other parameters, such as their masses. EOS estimation would therefore gain from exploring if the same EOS parameter values can explain consistently features in all parts of the waveform—specifically, the inspiral and the postmerger waveforms.

It is a pleasure to thank J. Clark, B. Lackey, and J. Read for reading the manuscript and providing useful input. Support comes from NSF Grants (No. PHY-1206108 and No. PHY-1506497); ERC Synergy Grant “BlackHoleCam” (No. 610058); “NewCompStar”; COST Action No. MP1304; the LOEWE Program in HIC for FAIR; the European Union’s Horizon 2020 Research and Innovation Programme (No. 671698) (call FETHPC-1-2014, project ExaHyPE); JSPS KAKENHI Grants (No. 15H06813 and No. 17K14305); and the Navajbai Ratan Tata Trust. The simulations were performed on SuperMUC at LRZ-Munich, on LOEWE at CSC-Frankfurt, and on Hazelhen at HLRS in Stuttgart.

Note added in proof.—Recently it was learned that the LIGO and Virgo detectors have observed gravitational waves from the binary neutron star GW170817 [40].

*sukanta@iucaa.in

- [1] B. P. Abbott, R. Abbott, T. D. Abbott, M. R. Abernathy, F. Acernese, K. Ackley, C. Adams, T. Adams, P. Addesso, R. X. Adhikari *et al.*, *Phys. Rev. Lett.* **116**, 061102 (2016).
- [2] E. E. Flanagan and T. Hinderer, *Phys. Rev. D* **77**, 021502 (2008).
- [3] R. Oechslin and H.-T. Janka, *Phys. Rev. Lett.* **99**, 121102 (2007).
- [4] A. Bauswein and H.-T. Janka, *Phys. Rev. Lett.* **108**, 011101 (2012).
- [5] L. Baiotti and L. Rezzolla, *Rep. Prog. Phys.* **80**, 096901 (2017).
- [6] J. Aasi *et al.* (LIGO Scientific Collaboration), *Classical Quantum Gravity* **32**, 074001 (2015).
- [7] F. Acernese *et al.* (VIRGO Collaboration), *Classical Quantum Gravity* **32**, 024001 (2015).
- [8] J. Abadie, B. P. Abbott, R. Abbott, M. Abernathy, T. Accadia, F. Acernese, C. Adams, R. Adhikari, P. Ajith, B. Allen *et al.*, *Classical Quantum Gravity* **27**, 173001 (2010).
- [9] W. Del Pozzo, T. G. F. Li, M. Agathos, C. Van Den Broeck, and S. Vitale, *Phys. Rev. Lett.* **111**, 071101 (2013).
- [10] M. Agathos, J. Meidam, W. Del Pozzo, T. G. F. Li, M. Tompitak, J. Veitch, S. Vitale, and C. Van Den Broeck, *Phys. Rev. D* **92**, 023012 (2015).
- [11] N. Stergioulas, A. Bauswein, K. Zagkouris, and H.-T. Janka, *Mon. Not. R. Astron. Soc.* **418**, 427 (2011).
- [12] K. Takami, L. Rezzolla, and L. Baiotti, *Phys. Rev. Lett.* **113**, 091104 (2014).
- [13] K. Takami, L. Rezzolla, and L. Baiotti, *Phys. Rev. D* **91**, 064001 (2015).
- [14] S. Bernuzzi, T. Dietrich, and A. Nagar, *Phys. Rev. Lett.* **115**, 091101 (2015).
- [15] J. S. Read, L. Baiotti, J. D. E. Creighton, J. L. Friedman, B. Giacomazzo, K. Kyutoku, C. Markakis, L. Rezzolla, M. Shibata, and K. Taniguchi, *Phys. Rev. D* **88**, 044042 (2013).
- [16] S. Bernuzzi, A. Nagar, S. Balmelli, T. Dietrich, and M. Ujevic, *Phys. Rev. Lett.* **112**, 201101 (2014).
- [17] L. Rezzolla and K. Takami, *Phys. Rev. D* **93**, 124051 (2016).
- [18] J. A. Clark, A. Bauswein, N. Stergioulas, and D. Shoemaker, *Classical Quantum Gravity* **33**, 085003 (2016).
- [19] K. Belczynski, S. Repetto, D. E. Holz, R. O’Shaughnessy, T. Bulik, E. Berti, C. Fryer, and M. Dominik, *Astrophys. J.* **819**, 108 (2016).
- [20] M. Dominik, E. Berti, R. O’Shaughnessy, I. Mandel, K. Belczynski, C. Fryer, D. E. Holz, T. Bulik, and F. Pannarale, *Astrophys. J.* **806**, 263 (2015).
- [21] S. E. de Mink and K. Belczynski, *Astrophys. J.* **814**, 58 (2015).
- [22] C. Kim, B. B. P. Perera, and M. A. Maura, *Mon. Not. R. Astron. Soc.* **448**, 928 (2015).
- [23] B. P. Abbott *et al.* (Virgo and LIGO Scientific Collaborations), *Astrophys. J.* **832**, L21 (2016).
- [24] C. Messenger, K. Takami, S. Gossan, L. Rezzolla, and B. S. Sathyaprakash, *Phys. Rev. X* **4**, 041004 (2014).
- [25] J. Clark, A. Bauswein, L. Cadonati, H.-T. Janka, C. Pankow, and N. Stergioulas, *Phys. Rev. D* **90**, 062004 (2014).
- [26] K. Hotokezaka, K. Kiuchi, K. Kyutoku, T. Muranushi, Y.-i. Sekiguchi, M. Shibata, and K. Taniguchi, *Phys. Rev. D* **88**, 044026 (2013).
- [27] See Supplemental Material at <http://link.aps.org/supplemental/10.1103/PhysRevLett.120.031102> for more details on the quasiuniversal relations and parameter-estimation methods employed in this work.
- [28] M. Punturo *et al.*, *Classical Quantum Gravity* **27**, 194002 (2010).
- [29] A. Akmal, V. R. Pandharipande, and D. G. Ravenhall, *Phys. Rev. C* **58**, 1804 (1998).

- [30] S. Ghosh and S. Bose, [arXiv:1308.6081](#).
- [31] A. Bauswein, H.-T. Janka, K. Hebeler, and A. Schwenk, *Phys. Rev. D* **86**, 063001 (2012).
- [32] LIGO Technical Report No. LIGO-T0900288-v3, 2010.
- [33] B. Farr *et al.*, *Astrophys. J.* **825**, 116 (2016).
- [34] S. Bernuzzi, T. Dietrich, W. Tichy, and B. Brügmann, *Phys. Rev. D* **89**, 104021 (2014).
- [35] W. Kastaun and F. Galeazzi, *Phys. Rev. D* **91**, 064027 (2015).
- [36] R. Valentim, E. Rangel, and J. Horvath, *Mon. Not. R. Astron. Soc.* **414**, 1427 (2011).
- [37] B. Kiziltan, A. Kottas, and S.E. Thorsett, [arXiv:1011.4291](#).
- [38] B. Kiziltan, *AIP Conf. Proc.* **1379**, 41 (2011).
- [39] B. Kiziltan, A. Kottas, M. De Yoreo, and S.E. Thorsett, *Astrophys. J.* **778**, 66 (2013).
- [40] B. P. Abbott *et al.* (Virgo, LIGO Scientific Collaboration), *Phys. Rev. Lett.* **119**, 161101 (2017).